



Investigation of Illite and Nano Illite for Efficient Removal of Cu (II), Ni (II), Zn (II), and Cd (II) Cations from Industrial Effluent

Ghada Sayed¹, Enas M. Abou-Taleb² and Fathy A. El-Saied³



¹ Department of Chemistry, Faculty of Science, Menoufia University, Shebin El Kom, Egypt

² Department of Water Pollution Research, National Research Centre, Cairo, Egypt

³ National Food Safety Authority, Cairo, Egypt

Abstract

This study investigated the potential of illite clay, sourced from New Valley, Egypt, for the removal of heavy metal ions (Cu(II), Ni(II), Zn(II), and Cd(II)) from industrial wastewater via an adsorption process. The experiment evaluated the adsorption behavior under various controlled conditions: varying metal ion concentration, adsorbent dosage, solution pH, and mixing time (at 500 rpm). Characterization of the illite and nanoillite clay employed Fourier Transform Infrared Spectroscopy (FTIR), Scanning Electron Microscopy (SEM), and Transmission Electron Microscopy (TEM). The results indicated rapid uptake by both illite and nanoillite, with maximum adsorption achieved within 90 minutes at room temperature (25°C) using an adsorbent dose of 0.3 mg/L and an initial metal concentration of 3 mg/L for all studied metal ions (Cu(II), Ni(II), Zn(II), and Cd(II)). Additionally, the adsorption isotherm data suggested a better fit with the second-order kinetic model, signifying the mechanism of adsorption. Finally, the effectiveness of illite/nanoillite clay was demonstrated by its application in removing metal ions from real-world industrial wastewater, leading to a significant reduction in their concentration. This approach addresses the environmental and health concerns associated with heavy metal pollution.

Keywords: Nanoparticles; Adsorption; Heavy metals; Kinetic; Isotherms; Illite; industrial wastewater

1. Introduction

In recent years, research has focused on the removal of heavy metals from aqueous solutions [1], ion exchange [2], chemical precipitation [3], phytoextraction [4], ultrafiltration, reverse osmosis, and electrodialysis [5] are just a few of the numerous methods for removing dissolved heavy metals [6]. Due to its high efficiency, ease of handling, availability of numerous adsorbents, and affordability, adsorption is typically chosen among all the water-treatment methods for the removal of heavy metal ions. Activated carbon is the most widely used adsorbent and is known for its high metal adsorption capability [7]. Although activated carbon is a useful tool for eliminating metal ions from wastewater, its use is costly and necessitates the addition of chelating chemicals to maximize its effectiveness, which drives up the cost of treatment [8]. Over the last twenty years, a lot of work has gone into finding affordable, efficient heavy metal adsorbents. Additionally, several natural materials and waste products have had their adsorption behavior examined [9]. These materials include agricultural by-products, microorganisms, and clay minerals [10]. The majority of these investigations have demonstrated that natural goods can function well as heavy metal adsorbents [11]. Heavy metal ions occur in many industrial activities, and this contamination causes a serious threat to the environment and human health, as these metals are non-biodegradable, toxic, even at low concentrations, and enter the food chain [12]. The accumulation of heavy metals in the human body causes brain, skin, pancreas, and heart diseases [13,14]. Heavy metals are classified as toxic and carcinogenic, they are capable of accumulating in tissues and cause diseases and disorders (Table 1).

Clay has shown capabilities in removing water contaminants such as chemicals [16, 17] and heavy metals [18]. More so, clay is inexpensive, abundant, widespread, and readily available. Other considerations are user-friendliness, cultural acceptability, and a low maintenance cost. Illite is a 2:1 clay mineral with very little tendency for interlayer swelling [19]. The adsorption process with illite depends on several factors, including pH, adsorbent content, initial adsorptive concentration, contact time, temperature, particle size, and ionic strength. In conventional methods, experiments are conducted by systematically varying the factors under study while holding the others constant. The main benefits are that not only can the effects of individual parameters be evaluated, but also their relative importance in a given process, as well as the ability to derive the interaction of two or more variables [20]. The objective of this study is to use illite as an adsorbent and then prepare nano Illite and use it to adsorb Cu(II), Ni(II), Zn(II), and Cd(II) ions from the water of industrial wastewater. We evaluated in detail the removal performance of Illite and nano Illite. Isotherm kinetic and thermodynamic modeling of the adsorption process was analyzed.

*Corresponding author e-mail: ghadasaid_2007@yahoo.com; (Ghada Sayed).

Receive Date: 14 May 2024, Revise Date: 05 July 2024, Accept Date: 15 July 2024

DOI: 10.21608/ejchem.2024.289013.9710

©2025 National Information and Documentation Center (NIDOC)

Table 1. Comparison of selected heavy metals, their anthropogenic sources, provisional maximum tolerable daily intake (PMTDI) according to WHO, and symptoms and diseases [15].

Heavy Metal	Anthropogenic Sources	PMTDI (mg/L)	Symptoms and Diseases References
Cd	Coal combustion, plastic stabilizers, nickel-cadmium batteries, petroleum refining, electroplating, and alloying industries.	0.003	Diabetes mellitus, nephropathy, emphysema, hypertension, and skeletal malformations.
Cu	mining activities, the production of paper, kitchenware, chemicals, and pharmaceuticals.	1.5	liver and eye damage, nausea, cramping, and convulsions Parkinson's, Wilson, Alzheimer's, Menkes illnesses.
Ni	Nickel steel, super alloys, non-ferrous alloys, electroplating, coinage, microphone capsules, rechargeable batteries, plumbing fixture plating, catalysts, and prosthetics for surgery and dentistry are some examples of these materials.	0.02	The symptoms include anemia, diarrhea, encephalopathy, hepatitis, lung and kidney damage, gastrointestinal discomfort, renal edema, pulmonary fibrosis, skin dermatitis, and malfunctions of the central nervous system.
Zn	Paints, cans, anti-corrosion coating, pigments, zinc alloys, rubber industry, and chemical industries	3	Depression, sluggishness, inability to breathe, appetite loss, diarrhea, migraines, electrolyte imbalance, dehydration, nausea and vertigo.

2. Material and Methods

2.1. Chemicals and instruments:

High-purity chemicals sourced from (Merck, Germany), were employed without additional purification. Stock solutions of Cu(II), Ni(II), Zn(II), and Cd(II) at a concentration of 1000 mg/L were prepared using the respective chlorides: CuCl₂, NiCl₂, ZnCl₂, and CdCl₂. To adjust the pH levels within the range of 1 to 9, we used 1.0 M hydrochloric acid and 1.0 M sodium hydroxide solutions. The final solution's pH was accurately measured with a German-made WTW-in-lab pH meter Metal ion concentrations in aqueous solutions were determined via Flame Atomic Absorption Spectroscopy (FAAS) utilizing a Perkin Elmer (503) instrument. A calibration curve was generated through standard metal ion solutions and analyzed using a Nicolet FT-IR spectrophotometer over a spectral range of 4000–400 cm⁻¹ as well as by Scanning Electron Microscopy (SEM) with equipment model (JSM-5300 from JEOL Ltd). To enhance conductivity during SEM analysis, gold coating was applied to the specimens following the (JEOL-JFC-1100E) sputtering procedure.

2.2 Experimental

Adsorbent

Illite was obtained from El Kharga, located in the New Valley Governorate in the Western Desert of Egypt.

Industrial wastewater

The industrial wastewater used in this study was collected from the Quesna industrial area, Menofia Governorate, Egypt. This site was chosen due to the high concentration of heavy metals in the wastewater from textile industries in this region. The experiments were carried out at the Faculty of Science, Menofia University.

2.2.1 Adsorbents Preparation

Hydrothermal method was employed for the preparation of nano-illite clay. Illite was first ground and suspended in distilled water to achieve a neutral pH 7 in the wash solution. Following purification, the sample was dried at 70°C for 24 hours. To achieve nano-illite, acid hydrolysis was then performed using a 60% sulfuric acid (H₂SO₄) solution at 45°C for 30 minutes with continuous stirring. The resulting nano-illite underwent repeated washing with distilled water to maintain a constant pH, followed by drying at 80°C for 24 hours. Finally, the material was rigorously crushed and sieved to obtain a uniform particle size of approximately 45 nm [21].

2.2.2 Optimal Conditions Determination

The study investigated the impact of contact time (10-120 minutes), solution pH (adjusted from 1 to 9 using 1.0 M HCl and 1.0 M NaOH), initial pollutant concentration (2-20 ppm), and adsorbent dosage (0.1-0.5 g) on the removal efficiency of illite and nano-illite adsorbents for textile wastewater treatment. After filtration with a 0.45-µm membrane, the remaining pollutant concentration was measured using atomic absorption spectroscopy to determine elimination percentage and adsorption capacity (calculated using equations S1 and S2 in the supplementary materials).

2.2.3 Adsorbents characterization

Fourier Transform Infrared Spectroscopy (FTIR) using a Shimadzu system (BX 0.8009) was used to analyze the functional groups within the synthesized adsorbent. The analysis covered a wavenumber range of 200-4000 cm⁻¹. Scanning Electron Microscopy (SEM) with a JEOL JSM-5300 instrument was used to examine the surface morphology of the adsorbent. The samples were sputter-coated with gold using a JEOL-JFC-1100E ion coater to enhance conductivity for SEM analysis. Transmission Electron Microscopy (TEM) with a JEOL Jem-1230 instrument was used to determine the adsorbent particle size.

Adsorption processes frequently combine physisorption, driven by weak van der Waals interactions, and chemisorption, involving stronger chemical bonds like ionic or covalent interactions. While electrostatic interactions between metal cations and electron-donating groups (hydroxyl, amine, carbonyl) can influence adsorption, physisorption primarily relies on dispersion forces and dipole-dipole interactions. Conversely, chemisorption can involve electron transfer or chelation, leading to significant electronic changes at the interface.[22]

Batch adsorption experiments were conducted to evaluate the effect of various factors on the adsorbent's capacity to remove metal ions. These factors included solution pH, contact time, adsorbent dosage, temperature, and initial metal ion concentration. The aim was to identify the optimal adsorption conditions [23].

Effect of Various Parameters:

The effect of each parameter (solution pH, adsorbent dosage, contact time, and initial metal ion concentration) on the adsorption process was investigated using separate experimental setups. Each experiment involved 50 mL of metal ion solution (predetermined concentration, adjusted to optimal pH if applicable) and varying amounts of the adsorbent (except for the dosage experiment). The mixtures were stirred for a specific time (except for the contact time experiment) at room temperature (25°C) and 500 rpm. The remaining metal concentration in the filtrate, after separation, was determined using Flame Atomic Absorption Spectroscopy (FAAS) to evaluate the adsorption efficiency.[24]

Effect of Initial Solution pH:

The impact of solution pH on metal ion removal was studied using a 50 mL metal ion solution (3 mg/L) with its pH adjusted between 1 and 9 using 1.0 M HCl and NaOH solutions.

Effect of Adsorbent Dosage:

The influence of adsorbent dosage was investigated using a 50 mL metal ion solution (3 mg/L, optimal pH) with varying adsorbent amounts (0.1-0.5 g).

Effect of Contact Time:

The effect of contact time was evaluated using a 50 mL metal ion solution (3 mg/L, optimal pH) with the optimal dose of adsorbent. The contact time was varied between 10 and 90 minutes.

Effect of Initial Metal Ion Concentration:

Individual containers, each containing 50 mL of solution with varying metal ion concentrations (2 to 20 mg/L), were prepared. The experiments were conducted under previously optimized conditions (pH, contact time, and adsorbent dosage). The remaining metal concentration in the solution was determined using FAAS after the experiment. This approach allowed assessment of the adsorption capacity at different initial metal ion concentrations.

Theoretical Modeling:

The following theoretical models were employed to analyze the experimental data obtained from the batch **adsorption Experiments:**

Adsorption Kinetics Models: Pseudo-first-order and pseudo-second-order kinetic models were used to fit the experimental data [25]. **Adsorption Equilibrium:** Langmuir and Freundlich isotherm models were applied to the data on initial metal ion concentrations to describe the adsorption equilibrium [26, 27].

3. Results and Discussion

3.1. Characterization of Adsorbent

Figure 1 shows the TEM image of the two adsorbents. The TEM image indicates that the particles of nano illite are more spherical, uniform, and mono-dispersed with less nanoparticle size (2 to 4 nm) than illite (20 to 30 nm). The SEM micrograph of illite and nano illite was carried out to analyse surface morphology. Figure 2, the SEM image shows that the surface has irregularly shaped pores that are suitable for adsorbing metal ions from liquids. The surface functional groups were characterized using FTIR (Fig. 3). Illite, an aluminum phyllosilicate, exhibited characteristic absorption bands in its IR spectrum. The most prominent peak at 912 cm^{-1} corresponds to the bending vibration of hydroxyl groups (OH) likely associated with Al-OH groups in the mineral structure. Another band at 1031 cm^{-1} signifies stretching vibrations within the tetrahedral Si-O units. This peak is consistent with the additional bands observed at 531 cm^{-1} and 470 cm^{-1} , which can be attributed to bending vibrations of Si-O-Al and Si-O-Si linkages, respectively. Finally, the broad bands at 3431 cm^{-1} and 1629 cm^{-1} indicate the presence of adsorbed water molecules on the illite surface. The stretching vibration at 3431 cm^{-1} and the bending vibration at 1629 cm^{-1} are characteristic of OH functionalities within these water molecules [28].

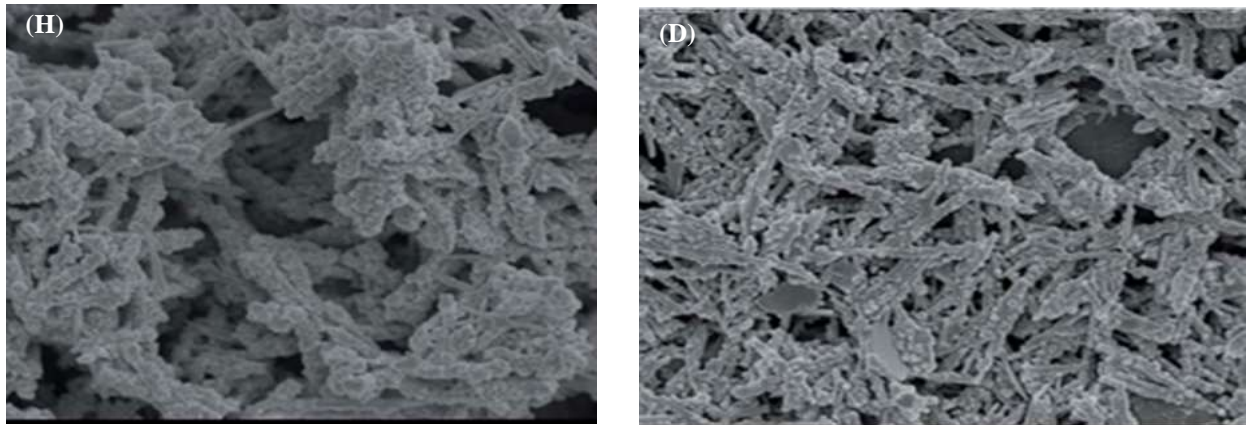


Figure 1: TEM image of d) illite and h) nano-illite.

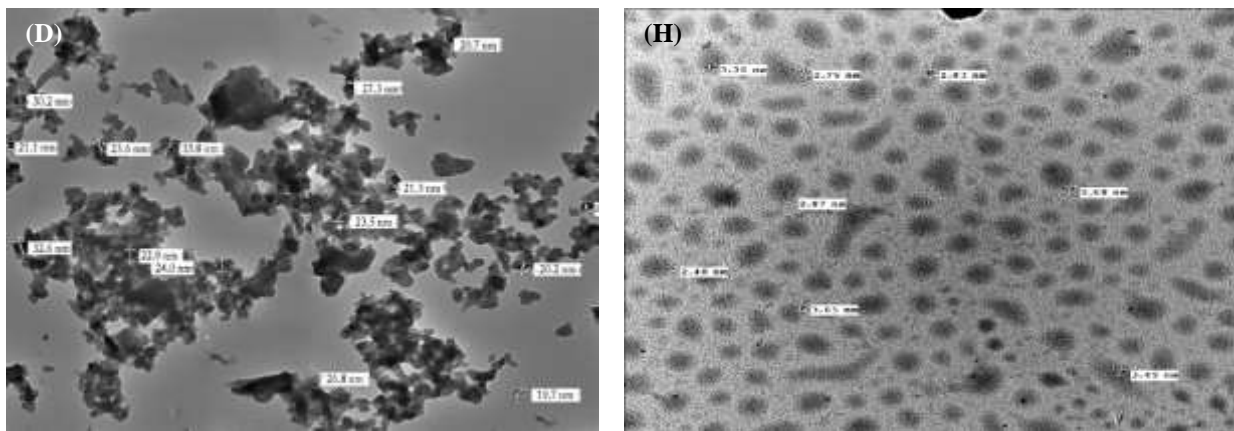


Figure 2: SEM image of d) illite and h) nano-illite.

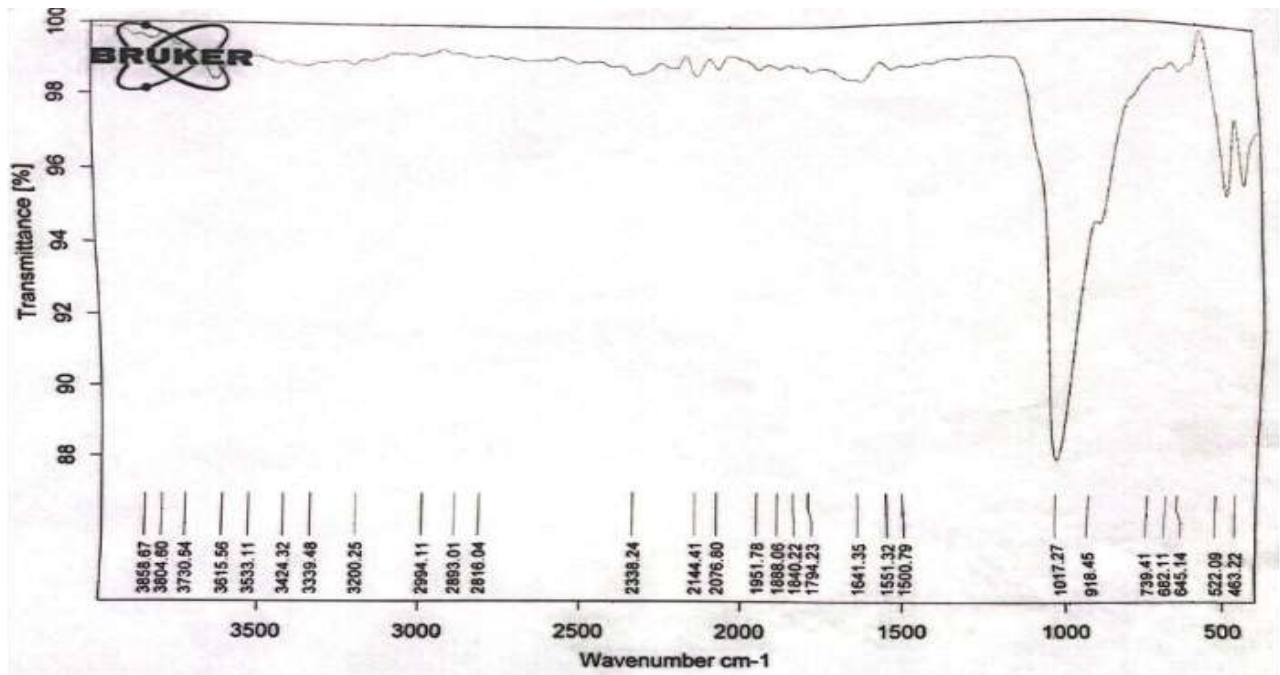


Figure 3: FTIR spectrum of adsorbents

3.2. Effect of pH on adsorption of metal ions

The effect of pH on Cu (II), Ni (II), Zn (II), and Cd (II) removal was investigated as shown in Figure 4. It was observed that the adsorption efficiency increased with increasing pH. The maximum removal of Cu (II) and Ni (II) on illite was respectively, 97% and 78% at (pH=6), and of Zn (II) and Cd (II) was respectively;73% and 87% at (pH=7). Where the maximum removal of Cu (II) and Ni (II) on nano illite was 98% and 80% at (pH=6) and of Zn (II) and Cd (II) was 80% and 91% at (pH=7). Since clay minerals generally possess electronegativity, cationic contaminants can be attracted and concentrated onto the clay's surface via the electrostatic interaction.

The electronegativity of clay has been confirmed to increase with increasing pH in solution, which is mainly attributed to the deprotonation of hydroxyls at high pH value. In contrast, a high concentration of H⁺ at a low pH value would reduce the negative charge on the clay's surface via protonation of hydroxyls [29], and the excess H⁺ would also compete with cationic contaminants to occupy the adsorption sites [30]. When the solution had a pH > 7.0, hydroxyl complexes of metal ions might form, limiting the activity by blocking the surface moieties and reducing adsorption performance [31].

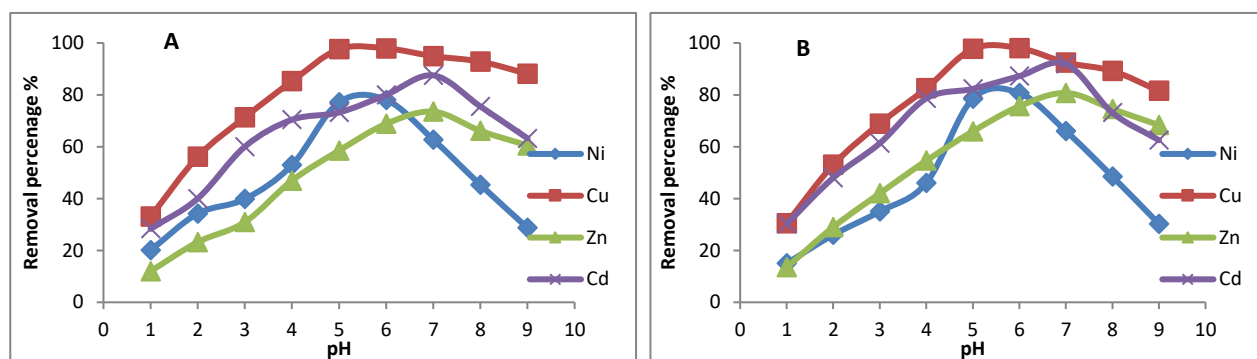


Figure 4: Effect of pH on removal percentage of metal ions (A) Illite and (B) nano-illite.

3.3. Effect of adsorbent dosage on adsorption of metals ions

The data for the removal percentages of Cu (II), Ni (II), Zn (II) and Cd (II) ions onto prepared adsorbents were illustrated in Figures 5. Generally, the removal is enhanced as the adsorbent dosage is increased due to the increase of reactive adsorption sites resulting in a rapid removal [32].

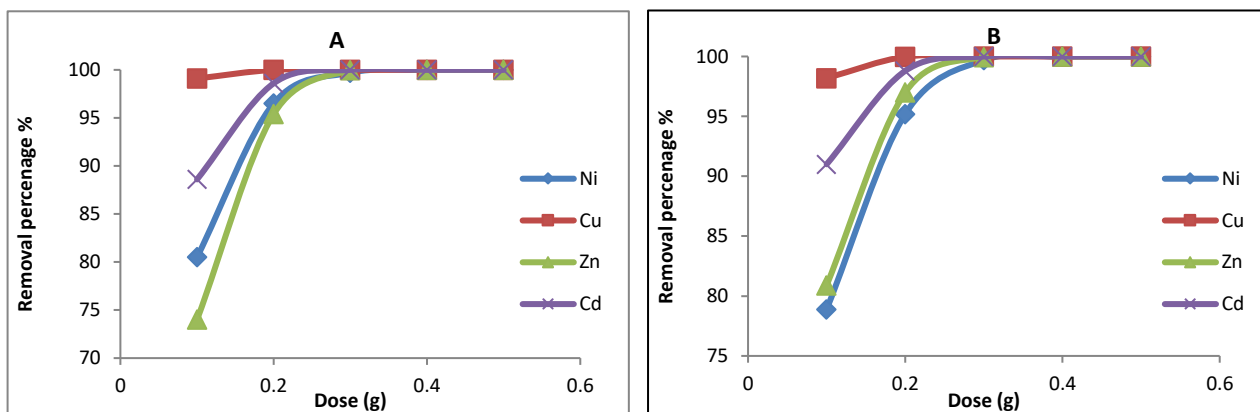


Figure 5: Effect of adsorbent dosage on removal percentage of metal ions on (A) illite and (B) nano-illite.

3.4. Effect of contact time on adsorption of metal ions

Figure 6 refers to the removal percentages of Cu (II), Ni (II), Zn (II), and Cd (II) ions onto illite and nano illite. The data recorded removal percentages of 53 %, 49 %, 47%, and 43 % for Cu (II), Ni (II), Zn (II), and Cd (II) ions, respectively onto illite and 56 %, 30 %, 50% and 45 % for Cu (II), Ni (II), Zn (II) and Cd (II) ions, respectively onto nano illite during the first 20 min. the percentage of metal ions removal reached 100 % within 90 min for all metal ions. The increase in the percentage of removal of the metal ions by increasing contact time is explained by the fact that during the initial stage of sorption, a large number of vacant surface sites are available for adsorption. After some time, the remaining vacant surface sites are difficult to be occupied due to saturation [33].

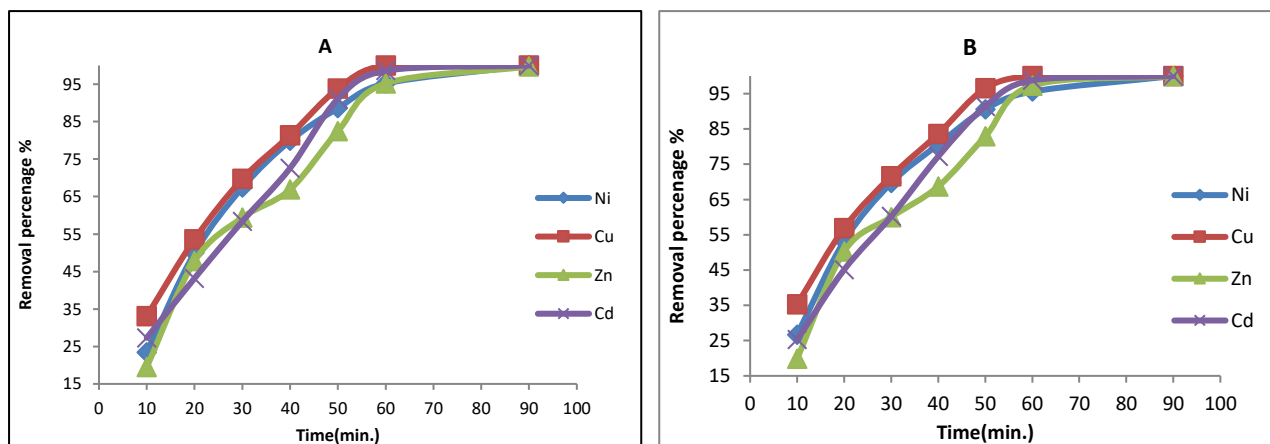


Figure 6: Effect of contact time on removal percentage of metal ions on (A) illite and (B) nano-illite.

3.5. Effect of initial heavy metal ion concentration on adsorption of metals ions

The obtained data are recorded in Figure 7. The lower the initial concentration is, the higher the percentage removal becomes. With the initial solution at a low concentration, the ratio between the number of ions and the number of adsorptive sites available is small; consequently, the adsorption sites are sufficient for contaminants, which can reach a high removal rate. As the concentration increases, increasing the probability of contacting with adsorption sites. As a result, the available sites are occupied and saturated rapidly. Due to the fixed amount of adsorption sites in adsorbents, the excess contaminants will remain in solution, causing the lower percentage removal [34]. The higher adsorption value of all metal ions is 100% for illite and nano illite, respectively at initial concentration ($C_0=3$ mg/L).

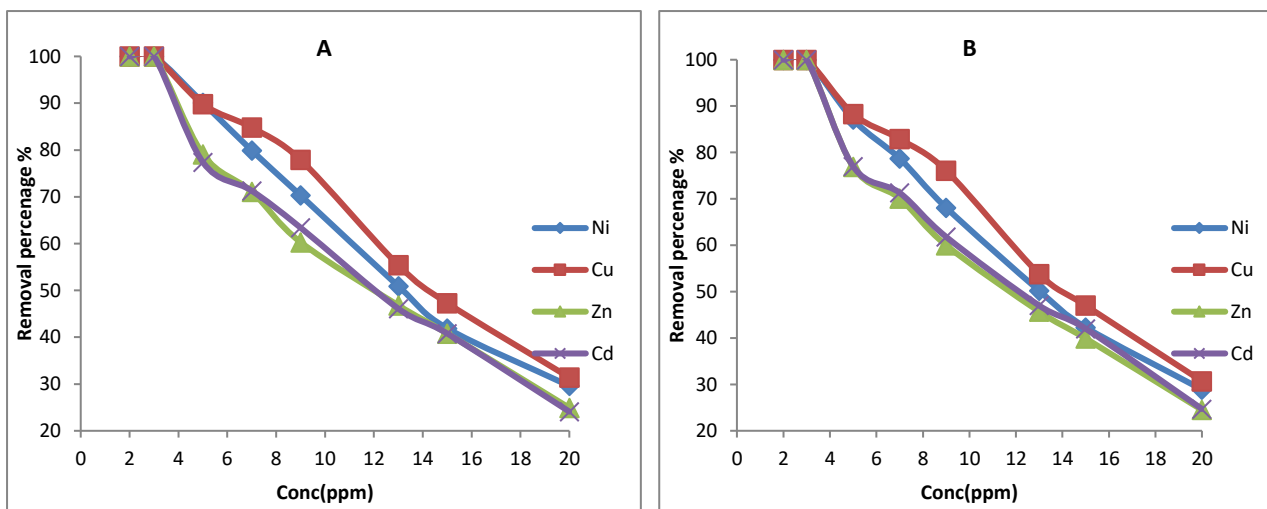


Figure 7: Effect of initial metal ion on removal percentage of metal ions on (A) illite and (B) nano-illite.

3.6. Adsorption kinetics

Adsorption is a physical-chemical process in which the mass transfers a solute (adsorbate) from the fluid phase to the surface of the adsorbent [35]. The kinetic adsorption of Cu (II), Ni (II), Zn (II), and Cd (II) on illite and nano Illite was fitted by pseudo-first-order and pseudo-second-order kinetic equations. The results are shown in Tables 2 and 3. Adsorption kinetics was investigated at different contact times and data was analyzed to know which model is better to explain the adsorption of Cu (II), Ni (II), Zn (II) and Cd (II) Figures 8 and 9 represent pseudo-first-order model and Figures 10 and 11 pseudo-second-order model for the ion.

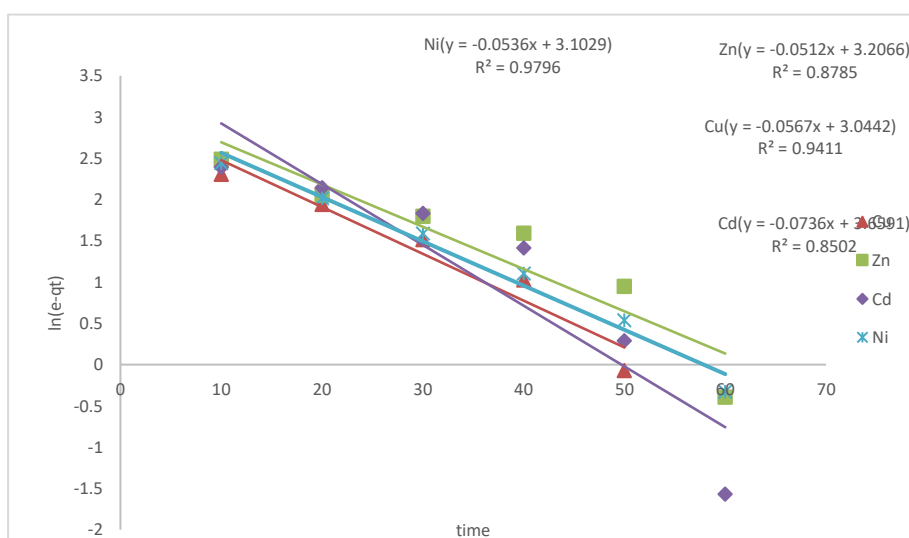


Figure 8: Pseudo-first-order reaction model for adsorption of metal ions on illite

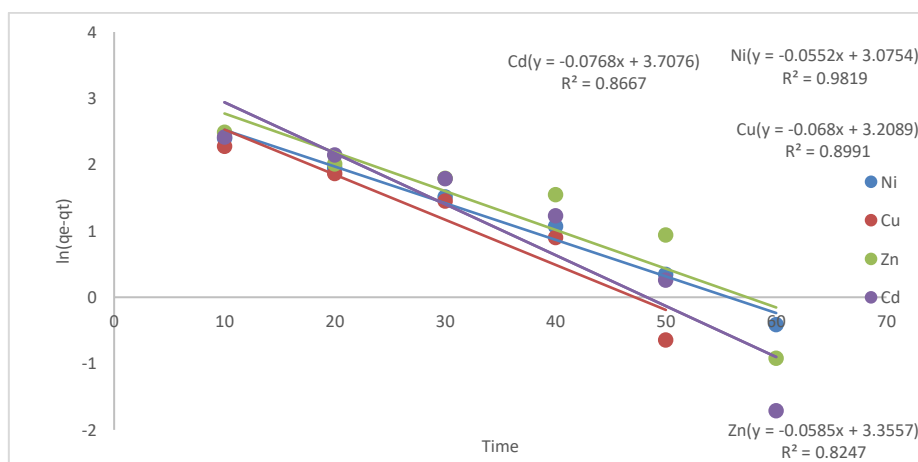


Figure 9: Pseudo-first-order reaction model for adsorption of metal ions on Nano illite

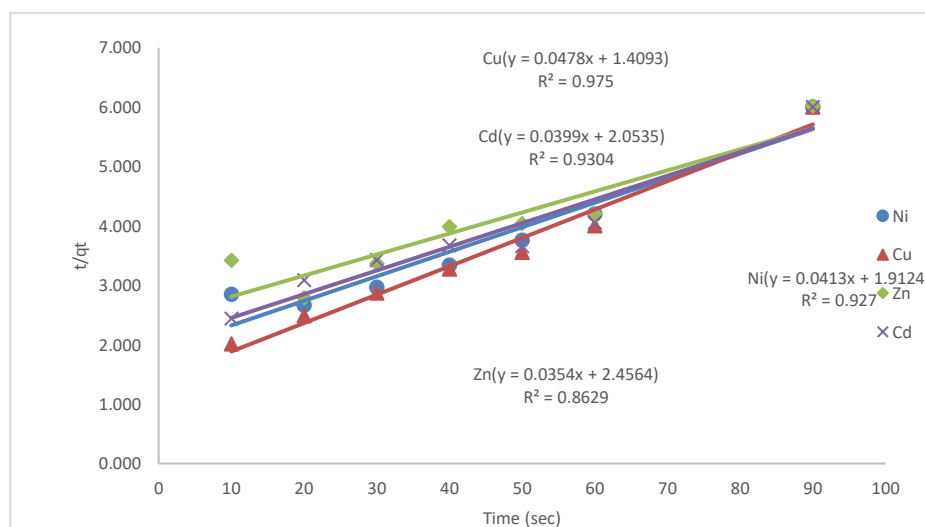


Figure 10: Pseudo-second-order reaction model for adsorption of metal ions on illite

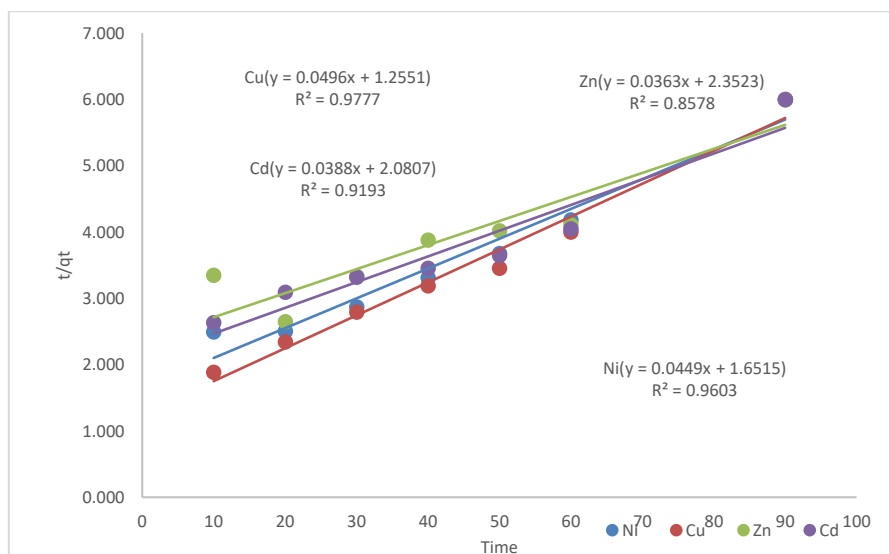


Figure 11: Pseudo-second-order reaction model for adsorption of metal ions on Nano illite

Table 2: Pseudo-first-order and Pseudo-second-order parameters for adsorption of metal ions on illite

Parameters	Ni (II)	Zn (II)	Cu (II)	Cd (II)	
					Parameters
Pseudo-first-order	K_1 (min^{-1})	0.054	0.051	0.057	0.074
	q_e cal.(mg/g)	25.658	28.665	24.751	40.755
	R^2	0.980	0.879	0.941	0.850
Pseudo-second-order	K_2 (g/mg min)	0.0012	0.0006	0.0020	0.0007
	q_e cal.(mg/g)	24.21	28.24	20.92	25.060
	R^2	0.987	0.893	0.975	0.930
Experimental	q_e Exp.(mg/g)	15.00	15.00	15.00	15.00

Table 3: Pseudo-first-order and Pseudo-second-order parameters for adsorption of metal ions on Nanoillite

Parameters	Ni (II)	Zn (II)	Cu (II)	Cd (II)	
					Parameters
Pseudo-first-order	K_1 (min^{-1})	0.055	0.058	0.068	0.077
	q_e cal.(mg/g)	22.658	28.665	24.751	40.755
	R^2	0.960	0.825	0.899	0.867
Pseudo-second-order	K_2 (g/mg min)	0.0012	0.0006	0.0020	0.0007
	q_e cal.(mg/g)	21.271	27.548	20.161	25.773
	R^2	0.982	0.858	0.978	0.919
Experimental	q_e Exp.(mg/g)	15.000	15.000	15.000	15.00

From the above data pseudo-second-order model yields very good straight lines as compared to pseudo-first-order because the correlation coefficient R^2 of pseudo-second-order model is greater than pseudo-first-order. The theoretical values of q_e of pseudo-second-order the model also agrees very well with the experimental ones. Both facts suggest that the adsorption of Cu (II), Ni (II), Zn (II), and Cd (II) ions on adsorbents follow the pseudo second-order kinetic model. This confirms that the predominant process here is chemisorption, which involves a sharing of electrons between the adsorbate and the surface of the adsorbent. Chemisorption is usually restricted to just one layer of molecules on the surface, although it may be followed by additional layers of physically adsorbed molecules [36].

3.7. Equilibrium Parameters of the Adsorption:

This study employed adsorption isotherms, mathematical models, to understand the interaction of Cu(II), Ni(II), Zn(II), and Cd(II) ions between the liquid and illite/nano-illite phases [37]. Langmuir and Freundlich models were used to analyze the equilibrium adsorption data. The Langmuir model assumes a uniform surface with a single layer (monolayer) of adsorbed metal ions on the adsorbent. This monolayer forms due to the equilibrium distribution of ions between the liquid and solid phases. Once this monolayer is established on the outer surface, no further adsorption is expected. Figures 12 and 13 depict the Langmuir

model for each ion by plotting the equilibrium concentration (C_e) divided by the amount adsorbed per gram of adsorbent (q_e) versus C_e . The Langmuir parameters, maximum monolayer adsorption capacity (q_{max}) and equilibrium constant (K_L), were determined from the slope and intercept of the plots, respectively.

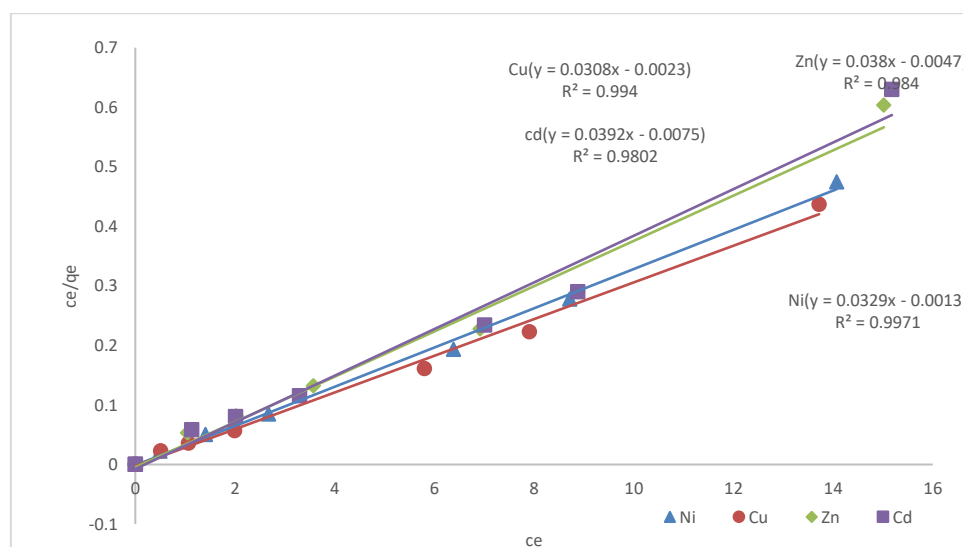


Figure 12: Langmuir adsorption isotherm model for adsorption of metal ions on illite

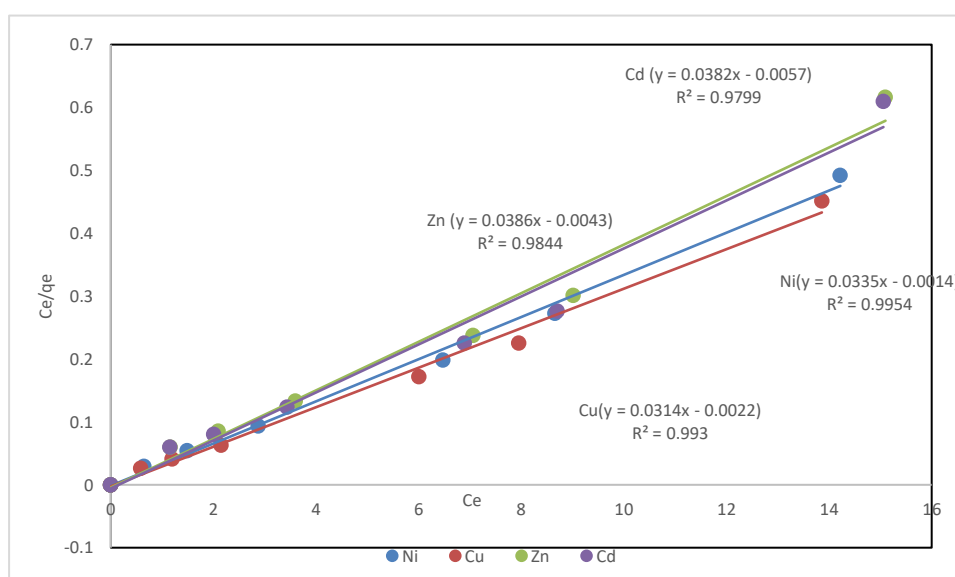


Figure 13: Langmuir adsorption isotherm model for adsorption of metal ions on nano illite

In contrast to the Langmuir model, the Freundlich isotherm offers an empirical approach, particularly suitable for heterogeneous surfaces [38]. This model emphasizes the role of surface heterogeneity in the adsorption process. Figures 14 and 15 depict the Freundlich model for each ion by plotting the logarithm of the amount adsorbed per gram of adsorbent ($\log q_e$) versus the logarithm of the equilibrium concentration ($\log C_e$). The Freundlich parameters, adsorption intensity ($1/n$), and Freundlich constant (K_F), were obtained from the slope and intercept of the plots, respectively. Here, $1/n$ reflects both the energy distribution and the heterogeneity of the adsorption sites.

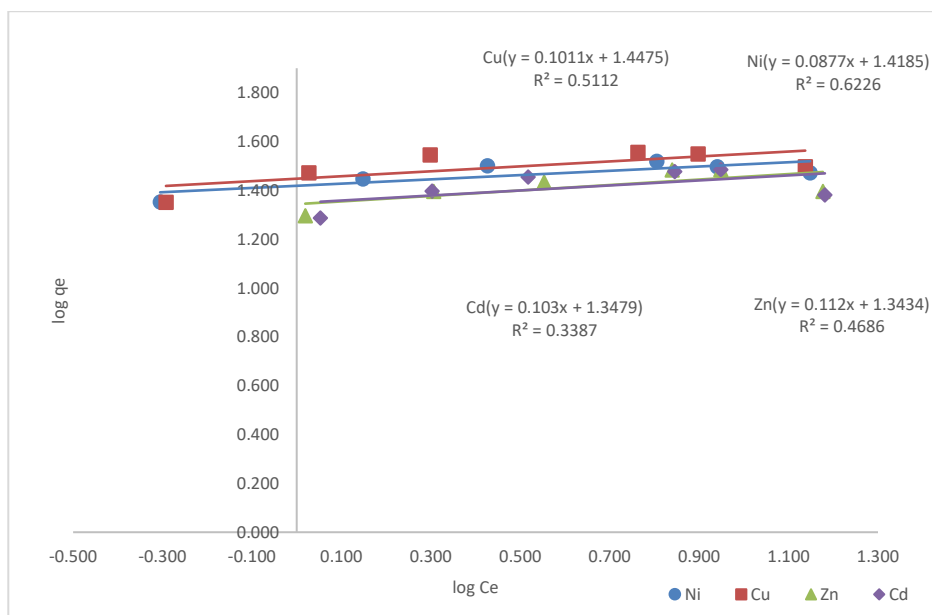


Figure 14: Freundlich adsorption isotherm model for adsorption of metal ions on illite

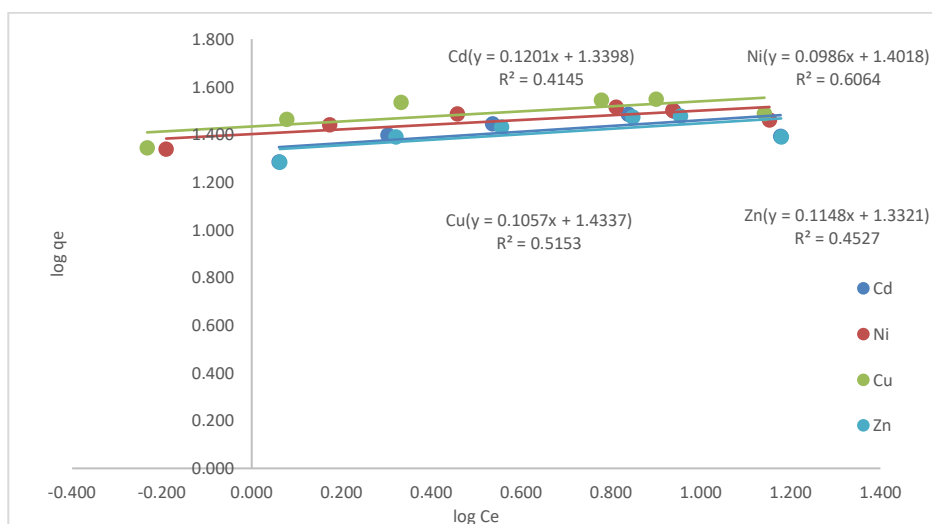


Figure 15: Freundlich adsorption isotherm model for adsorption of metal ions on nanoillite.

Table 4: Langmuir and Freundlich adsorption isotherm parameters for adsorption of metal ions on illite

	Parameters	Ni(II)	Zn (II)	Cu (II)	Cd (II)
Langmuir	K_L (L/mg)	25.310	8.080	16.520	5.220
	q_{max} mg/g)	30.390	26.320	26.310	25.510
	R_L	0.002	0.006	0.003	0.007
	R^2	0.997	0.984	0.994	0.980
Freundlich	K_F (L/g)	25.220	21.480	27.140	21.860
	$1/n$	0.088	0.112	0.101	0.103
	R^2	0.623	0.469	0.511	0.339

Table 5: Langmuir and Freundlich adsorption isotherm parameters for adsorption of metal ions on nano illite

Parameters	Ni (II)	Zn (II)	Cu (II)	Cd (II)
	K_L (L/mg)	23.920	8.970	14.270
q_{max} (mg/g)	29.850	25.910	31.840	26.180
R_L	0.002	0.005	0.003	0.007
R^2	0.995	0.984	0.993	0.980
K_F (L/g)	25.220	21.480	27.140	21.860
$1/n$	0.099	0.115	0.106	0.120
R^2	0.606	0.453	0.515	0.415

The analysis of the data suggests favorable adsorption for all the studied metal ions (Cu(II), Ni(II), Zn(II), and Cd(II)) based on both the Langmuir and Freundlich models. This favorability is indicated by R_L values (Langmuir) greater than zero and less than one, and n values (Freundlich) between 0.1 and 1 in both models. However, the Langmuir model exhibited a higher R^2 value compared to the Freundlich model. This signifies that the adsorption process follows the Langmuir isotherm model. This implies a homogenous surface with monolayer adsorption of metal ions, where there's minimal interaction between the adsorbed species [39].

3.8. Application to industrial wastewater:

To apply the treatment method used for removing Cu (II), Ni (II), Zn (II), and Cd (II) ions from synthetic water, a wastewater sample was collected from a textile factory located in an industrial area, Quesne, El Menoufia Governorate, Egypt. The sample was passed through a 0.45 μ m membrane filter. The metal concentration in the wastewater sample was determined by a flame atomic absorption spectrophotometer. According to batch experimental results of the removal of Cu (II), Ni (II), Zn (II), and Cd (II) ions from synthetic water, the optimum treatment conditions were pH = 7, adsorbent dose = 0.3g and contact time = 90 min. In the experiment, 0.3 g of each adsorbent was added to 50 mL of wastewater sample and shaken at 500 rpm at room temperature (25 °C) for 90 min at pH 7. Suspensions were filtered using 0.45 μ m membrane filter paper and kept for metal analyses.

Table 6: Adsorption of metal cations from Industrial wastewater using illite and nano illite

Metal ions	Concentration (mg/L) before treatment	Concentration (mg/L) After treatment		Removal percentage %		Detection limit
		illite	nano-illite	illite	nano-illite	
Zn (II)	2.356	<0.005	<0.005	100%	100%	0.005
Cu (II)	3.977	<0.01	<0.01	100%	100%	0.01
Cd (II)	1.213	<0.002	<0.002	100%	100%	0.002
Ni (II)	0.654	<0.02	<0.02	100%	100%	0.02

4. Conclusions

This investigation explored the potential of illite and nano-illite for the removal of copper (Cu(II)), nickel (Ni(II)), zinc (Zn(II)), and cadmium (Cd(II)) ions from aqueous solutions. Batch adsorption experiments were conducted to elucidate the influence of contact time, initial metal concentration, adsorbent dosage, and pH on removal efficiency. The results indicated that Cu(II) and Ni(II) exhibited optimal adsorption at pH 6, while Zn(II) and Cd(II) demonstrated higher removal at pH 7. An adsorbent dosage of 0.3 g was determined to be most effective for all metal ions. Equilibrium removal for all metal ions was achieved within 90 minutes of contact time. The Langmuir and pseudo-second-order kinetic models provided the best fit for the isotherm and kinetic data, respectively, suggesting monolayer chemisorption of the metal ions onto the illite and nano-illite surfaces.

Significantly, reducing clay particle size to the nanoscale resulted in a pronounced enhancement of adsorption capacity. This can be attributed to the increased surface area and unique charge properties inherent to nanomaterials [40, 41]. Interestingly, the comparable q_{max} values for all elements across Tables 4 and 5 suggest similar adsorption behavior for both illite and nano-illite. This implies that the selection of illite or nano-illite may not significantly impact removal efficiency. Consequently, the cost associated with the conversion of all clays to nano-illite might be unnecessary. A more cost-effective approach could be to prioritize the element with more favorable characteristics, such as abundance or ease of processing.

This approach, which leverages the natural properties of clays, holds promise for the development of efficient and cost-effective adsorbents for water purification applications.

Conflicts of interest

There is no conflict of interest.

References

- [1] C. Li, H. Wang, X. Liao, R. Xiao, K. Liu, J. Bai, B. Li, Q. He, Heavy metal pollution in coastal wetlands: A systematic review of studies globally over the past three decades, *Journal of Hazardous Materials*. 424(2022) 127312.
- [2] M. Zaynab, R. Al-Yahyai, A. Ameen, Y. Sharif, L. Ali, M. Fatim, K. AliKhan, S. Li, Health and environmental effects of heavy metals. *Journal of King Saud University - Science*. 34 (2022) 101653
- [3] A. T. Hoang, S. Nižetić, C. K. Cheng, R. Luque, S. Thomas, T. L. Binh, V. VietPham, X. P. Nguyen, Heavy metal removal by biomass-derived carbon nanotubes as a greener environmental remediation: A comprehensive review, *Chemosphere*. 287 (2022) 131959.
- [4] H. G. Hoang, C. F. Chiang, C. Lin, C. Y. Wu, C. W. Lee, N. K. Cheruiyot, H. T. Tran, X. T. Bu, Human health risk simulation and assessment of heavy metal contamination in a river affected by industrial activities, *Environmental Pollution*. 285 (2021) 117414.
- [5] A. Jawed, V. Saxena, L.M. Pandey, Engineered nanomaterials and their surface functionalization for the removal of heavy metals: a review. *J Water Process Eng* 33(2020) 101009.
- [6] X. Zhang, Y. Dou, C. Gao, C. He, J. Gao, S. Zhao, L. Deng, Removal of Cd(II) by modified maifanite coated with Mg-layered double hydroxides in constructed rapid infiltration systems, *Sci. Total Environ*. 685 (2019) 951–962.
- [7] C.F. Mhina, H.Y. Jung, J.K. Kim, Recovery of antioxidant and antimicrobial peptides through the reutilization of Nile perch wastewater by biodegradation using two *Bacillus* species, *Chemosphere*. 253 (2020) 126728.
- [8] I. Lee, C.W. Park, S.S. Yoon, H.M. Yang, Facile synthesis of copper ferrocyanide-embedded magnetic hydrogel beads for the enhanced removal of cesium from water, *Chemosphere*. 224 (2019) 776–785.
- [9] Y. Zhao, S. Kang, L. Qin, W. Wang, T. Zhang, S. Song, S. Komarneni, Self assembled gels of Fe-chitosan/montmorillonite nano sheets: Dye degradation by the synergistic effect of adsorption and photo-Fenton reaction, *Chem. Eng. J.*379 (2020) 122322.
- [10] W. Liu, D. Wang, R.A. Soomro, F. Fu, N. Qiao, Y. Yu, R. Wang, B. Xu, Ceramic supported attapulgite- graphene oxide composite membrane for efficient removal of heavy metal contamination, *J. Memb. Sci.* 591 (2019)117323.
- [11] W. Peng, H. Li, Y. Liu, S. Song, A review on heavy metal ions adsorption from water by graphene oxide and its composites, *J. Mol. Liq.* 230 (2017) 496–504.
- [12] A.E. Burakov, E.V. Galunin, I.V. Burakova, A.E. Kucherova, S. Agarwal, A.G. Tkachev, V.K. Gupta, Adsorption of heavy metals on conventional and nanostructured materials for wastewater treatment purposes: A review. *Ecotoxicol. Environ. Saf.*, 148 (2018) 702–712.
- [13] K.U. Mohammad, A review on the adsorption of heavy metals by clay minerals, with special focus on the past decade. *Chem. Eng. J.* 308(2017) 438–462.
- [14] V. Masindi, W.M. Gitari, Simultaneous removal of metal species from acidic aqueous solutions using cryptocrystalline magnesite/bentonite clay composite: An experimental and modelling approach. *J. Clean. Prod.*, 112 (2016) 1077–1085.
- [15] M.M. Haemmerle, J. Fendrych, E. Matiassek, C. Tschegg, Adsorption and release characteristics of purified and non-purified clinoptilolite tuffs towards health-relevant heavy metals, *Crystals*, 11(11) (2021)1343.
- [16] G.M. Joziane, P.M. Murilo, K. Thirugnanasambandham, H.B.F. Sergio, L.G. Marcelino, A.S.D.B. Maria, V. Sivakumar, Preparation and characterization of calcium treated bentonite clay and its application for the removal of lead and cadmium ions: Adsorption and thermodynamic modeling. *Process Saf. Environ.*, 111(2017)244–252.
- [17] A. Sari, M. Tuzen, Cd(II) adsorption from aqueous solution by raw and modified kaolinite. *Appl. Clay Sci.* 88–89(2014)63–72.
- [18] A.M. Atta, H.A. Al-Lohedan, Z.A. AlOthman, A.A. Abdel-Khalek, A.M. Tawfeek, Characterization of reactive amphiphilic montmorillonite nanogels and its application for removal of toxic cationic dye and heavy metals water pollutants. *J. Ind. Eng. Chem.*, 31(2015) 374–384.
- [19] S.S. Yuan, Z.Y. Li, Z.D. Pan, Y.M. Wang, Removal of copper and cadmium ions in aqueous solution via adsorption by Nano-sized Illite-Smectite Clay. *J. Chin. Ceram. Soc.*, 44(2016) 43–49.
- [20] L.H. Zhang, Y.H. Yuan, Z.G. Yan, Y.Y. Zhou, C.Y. Zhang, Y. Huang, M. Xu, Application of nano illite/smectite clay for adsorptive removal of metals in water. *Res. Environ. Sci.*, 29(2016)115–123.
- [21] A. H. Mangood, F. A. El-Saied, F. H. El-shinawy, and S. A. Abo-Elenan, "Metals Removal from Contaminated Aqueous Medium by Using Modified Cellulose-N(4)-Antipyrinyl Thiosemicarbazide," *Polycyclic Aromatic Compounds*, 44(3)(2024)1760-1780.
- [22] W. Thabet, S. Ahmed, O. Abdelwahab, and N. O. Soliman, "Enhancement Adsorption of Lead and Cadmium Ions From Waste Solutions Using Chemically Modified Palmfibers" *Egyptian Journal of Chemistry*, 63(12)(2020)4917-4927. doi: 10.21608/ejchem.2020.31220.2663
- [23] M. Anjum, R. Miandad, M. Waqas, F. Gehany, M.A. Barakat, Remediation of waste water using various nano-materials, *Arabian Journal of Chemistry* 12(8)(2019) 4897–4949
- [24] S. Lagergren, Zur theorie der sogenannten adsorption gelöster stoffe (about the theory of so-called adsorption of soluble substances); *Kungliga Svenska Vetenskapsakademiens (Royal Swedish Academy of Sciences): Stockholm, Sweden*, (1898)1–39.
- [25] Y.S. Ho, G. McKay, Pseudo-second order model for sorption processes. *Process Biochem*, 34(1999)451–465.

- [26] I. Langmuir, The adsorption of gases on plane surfaces of glass, mica and platinum. *J. Am. Chem. Soc.*, 40(1918)1361–1403.
- [27] H.M.F. Freundlich., Über die adsorption in lösungen. *Z. Phys. Chem.*, 57 (1906) 385–470.
- [28] G. Sayed, E. M. A. Taleb, and F. A. El-Saied, Adsorption of Ca (II), Mn (II), Fe (III), Mg (II), and Pb (II) Ions from New Valley Groundwater Using Illite and Nanoparticles, *Am. J. Environ. Clim.*,3(1)(2023)1-10.
- [29] D. Haldhar, S. Sahoo and P. C. Mishra, Adsorption of As(III) from aqueous solution by groundnut shell, *Indian Journal of Applied Research*. 4 (2014) 270-273.
- [30] C. Liu, A.M. Omer, X. kun Ouyang, Adsorptive removal of cationic methylene blue dye using carboxymethyl cellulose/k-carrageenan/activated montmorillonite composite beads: Isotherm and kinetic studies, *Int. J. Biol. Macromol.* 106 (2018) 823–833.
- [31] W. Wang, Y. Zhao, H. Yi, T. Chen, S. Kang, T. Zhang, F. Rao, S. Song, Pb(II) removal from water using porous hydrogel of chitosan-2D montmorillonite, *Int. J. Biol. Macromol.* 128 (2019) 85–93.
- [32] S. Wadhawan, A. Jain, J. Nayyar, S.K. Mehta, Role of nanomaterials as adsorbents in heavy metal ion removal from waste water: a review. *J Water Process Eng.* 33 (2020)101038.
- [33] T. K. Sen and D. Gomez, Adsorption of zinc (Zn²⁺) from aqueous solution on natural bentonite, *Desalination*. 267 (2011) 286-294. 25 h.
- [34] E. Igberase, P. Osifo, and A. Ofomaja, The adsorption of Pb, Zn, Cu, Ni, and Cd by modified ligand in a single component aqueous solution: equilibrium, kinetic, thermodynamic, and desorption studies, *International Journal of Analytical Chemistry*. (2017) 15(2017) 29.
- [35] T. Ngulube, J.R. Gumbo, V. Masindi, A. Maity, An update on synthetic dyes adsorption onto clay based minerals: A state-of-art review, *J. Environ. Manage.* 191 (2017) 35–57.
- [36] S. P. Silva, S. Sousa and J. Rodrigues, Adsorption of Acid Orange 7Dye in Aqueous Solutions by Spent Brewery Grains, *Journal of Separation and Purification Technology*. 40 (2004) 309–315.
- [37] E. N. El Qada, S. J. Allen and G. M. Walker, Adsorption of methylene blue onto activated carbon produced from steam activated bituminous coal: a study of equilibrium adsorption isotherm, *Chemical Engineering Journal*. 124 (2006) 103–110.
- [38] M. M. Ghoniem, H. S. El-Desoky, K. M. El-Moselhy, A. Amer, E. H. AboEl-Naga, L. I. Mohamedein and A. E. Al-Prol. Removal of cadmium from aqueous solution using green marine algae, *Ulva lactuca*. *Egypt Journal of Aquatic Research*. 40 (2014) 235–242.
- [39] S.A. Shama and M. A. Gad, Removal of heavy metals (Fe³⁺, Cu²⁺, Zn²⁺, Pb²⁺, Cr³⁺ and Cd²⁺) from aqueous solutions by using hebbra clay and activated carbon. *Journal of Portugaliae Electrochimica Acta*. 28(2010) 231–239.
- [40] F. A. El-Saied, S. Abo- El-Enein, F. El-shinawy, Removal of lead and copper ions from polluted aqueous solutions using nano-sawdust particles, *International J. of waste resources*. 7(2017) 1000305-1000311.
- [41] F. Fareed, M. Ibrar, Y. Ayub, R. Nazir, and L. Tahir, "Clay-Based Nanocomposites: Potential Materials for Water Treatment Applications," in *Advanced Research in Nanosciences for Water Technology*. Nanotechnology in the Life Sciences, R. Prasad and T. Karchiyappan, Eds. Springer, Cham, 2019, pp. 189-212. [Online]. Available: https://doi.org/10.1007/978-3-030-02381-2_10